Wireless Pers Commun (2017) 94:1105–1121
DOI 10.1007/s11277-016-3673-2

High-Speed Positioning and Automatic Updating Technique Using Wi-Fi and UWB in a Ship

Ju-Hyeon Seong[1] · Eun-Chang Choi[2] · Jang-Se Lee[3] · Dong-Hoan Seo[4]

Published online: 3 September 2016

Abstract Wi-Fi-based fingerprint indoor localization is widely used owing to its low cost and the rapid increase of its network, even though this method requires radio map creation and maintenance which accompany time-consuming and continuous monitoring. Considering these advantages and limitations and the fact that conditions in a ship are more likely to suffer from scattered and distorted wireless signals caused by a special structure of ship, this paper presents an efficient shipboard positioning technique using existing shipboard Wi-Fi network and additional ultra-wide band (UWB) nodes which are the IEEE 802.15.4a modules capable of precise positioning. The proposed method can reduce computational complexity that can occur during signal acquisition and automatically create and update more rapid and precise modified radio maps, by fusing the distance information obtained from UWB and Wi-Fi fingerprint. In addition, the advantages of proposed system are that selective computation technique which can remove weak signals is applied to reduce the amount of computation needed to create modified radio map and the positioning errors can be improved by assigning a positioning weight to each preceding position value because the same signal intensities can occur in other areas within the Wi-Fi network. The efficiency of the proposed method and its comparison with other methods are demonstrated.

Keywords Wi-Fi · Fingerprint · UWB · Shipboard · Radio map

✉ Dong-Hoan Seo
dhseo@kmou.ac.kr

[1] Department of Electrical and Electronics Engineering, Korea Maritime and Ocean University, #727 Taejong-Ro, Youngdo-Gu, Busan 49112, Korea

[2] Medical IT Convergence Research Section, Electronics and Telecommunications Research Institute, #1 Techno sunhwan-Ro 10-Gil, Yuga-myeon, Dalseong-Gun, Deagu 42994, Korea

[3] Division of Marine Information Technology, Korea Maritime and Ocean University, #727 Taejong-Ro, Youngdo-Gu, Busan 49112, Korea

[4] Division of Electronics and Electrical Information Engineering, Korea Maritime and Ocean University, #727 Taejong-Ro, Youngdo-Gu, Busan 49112, Korea

1 Introduction

Currently, various localization systems using a wireless communication technology, which provide useful information to users by recognizing the position of objects, have been widely applied in various areas such as logistical and industrial fields. Especially, an indoor positioning system has been introduced, which can guide a user to a desired destination in a complicated indoor environment, where the global positioning system (GPS) is not available. Among such techniques, indoor positioning technology that uses RSSI-based wireless local area network (WLAN) can estimate the distance values between fixed nodes and moving nodes carried by objects. This technology can measure distances only in an obstacle-free line-of-sight (LOS) environment because of its high signal attenuation induced by obstacles [1, 2]. In indoor environments with limited area and many obstacles, it is difficult to apply positioning systems based on the RSSI-to-distance ratio. Meanwhile, the Wi-Fi fingerprint method is generally used for indoor environments because of its consistent performance irrespective of obstacle-induced received signal strength intensity (RSSI) attenuation that is likely to occur in non-LOS (NLOS) environments, where the transmitted signal blocking can be occurred by obstacles such as wall, door, and furniture [3–7].

The fingerprint technique is divided into two schemes according to whether the collection of RSSIs in the radio map is made from known access point (AP) locations or unknown ones. In the former scheme, error reduction is possible via adjustment depending on LOS or NLOS environment. However, this method requires a prior determination of all AP positions in order to implement the initial positioning system, even afterwards and a constant updating of AP positions which is necessary each time the number or information of their positions is changed. On the other hand, whereas collecting RSSIs without knowing AP locations facilitates the rapid creation of radio maps, such maps are vulnerable to the AP changes caused by the presence or absence of obstacle-related conditions because it depends only on the intensity of AP signals. In particular, if smartphones are used instead of producing hardware for RSSI measurements, RSSIs received from APs might be subject to considerable fluctuations, leading to low accuracy and inconsistent RSSI. To reduce this problem, some of methods have been suggested in which radio maps are generated through mean values, weights, or maximum likelihood estimation (MLE) [8–12].

More recently, Liu et al. [13] proposed a peer assisted localization approach to obtain accurate acoustic ranging estimates among peer smartphones in Wi-Fi environment. This method based on the information of peripheral smartphones aimed to reduce the position estimation error due to the fluctuations of the measured RSSIs. However, this method in an NLOS environment is likely to incur considerable RSSI errors depending on the presence or absence of obstacles and surrounding structures compared to the fingerprint method. Muller et al. [14] proposed a positioning algorithm that uses UWB and Bayesian filtering method in order to resolve the problem of high computational burden imposed by Gaussian mixtures (GM) and particle filters. A feasible positioning model in this method requires the acquisition process for accurate information on the initial positions in order to reduce continuous errors caused by incorrect initial values. Ahmed et al. [15], based on statistical anomaly detection techniques and particle filtering to implement a WLAN indoor positioning system, proposed a positioning scheme robust to environmental changes and requiring significantly lower deployment overhead. However, using more than two probabilistic algorithms with high computational burdens, such as particle filters, this system is

likely to incur loads when tracking multiple objects. As described above, most studies have traditionally focused on positioning technologies inside buildings, and various filters used for enhancing object tracking do not yield accuracy below 1 m and some of them require large computational burdens. Specifically, these techniques are difficult to apply appropriately in areas such as passenger ships which consist of narrow aisle, steel structure, engine room, etc. that can deteriorate the accuracy of location estimation. In addition, because most passengers who are unfamiliar with these complicated structures, unlike a large building or convention center in land, are difficult to effectively respond to an emergency situation such as fire or wreck, positioning technologies which are suitable in ship environment are required.

Against these backdrops, this paper proposes a shipboard positioning system that combines TOF-based UWB with fingerprint using Wi-Fi network which is currently applied to ship. The proposed algorithm can substantially reduce standby time and positioning errors because the proposed radio map is modified by the distance information measured from a fixed UWB nodes and a moving UWB node unlike traditional fingerprint method. In addition, this algorithm enables a continuous automatic update of the modified radio map on the basis of the UWB distance estimation, and the positioning errors and computation time can be reduced by performing selective computations and applying a weighted filter using each preceding estimated value, respectively.

2 Related Work

2.1 Wi-Fi Based Fingerprint Technique

Fingerprint is one of the Wi-Fi-based positioning technologies. Its tracking accuracy is higher than that of RSSI-based time-of-arrival (TOA) technique because it estimates positions by analyzing and comparing RSSIs that reach the measurement area independently of interior structures. This technology consists of two phases: (1) training phase, in which a radio map is set up by collecting AP information, including the service set identification (SSID) and RSSI of the AP measured at the reference points placed at intervals of 3–5 m in the area to be covered; (2) positioning phase, in which positions are estimated by comparing the signal intensities between the database established in the training phase and the signals measured at the receiver.

In the training phase, the area to be measured is divided at regular intervals, depending on the indoor environment, and the reference points are thus set up. All AP signals measured at each reference point are then collected and used to create a radio map based on the RSSIs that match each reference point. This process of collecting all AP signals emitted from each pre-determined reference point usually requires a considerable length of time because of APs whose receiving rates are extremely low depending on device-dependent receiving conditions, or on position-dependent signal intensities when measuring the RSSI of APs. Let a given interior point be i and each of AP signals collected at position i be expressed as AP_1, AP_2, AP_3, …, AP_n; then, all the signal P^i received at position i can be expressed as follows:

$$P^i = [AP_1, AP_2, AP_3, \ldots, AP_n] \tag{1}$$

Thus, a radio map of the area to be covered is a set which is created with the values P^i collected in accordance with each position i. Based on the radio map created in the training

phase, computations are performed in the positioning phase by comparing real time measured RSSI of Wi-Fi APs with the same ones of stored in the radio map and Euclidean distance is extracted. With all radio maps created in the area to be estimated, the Wi-Fi AP signals (P^i_{real}) measured to estimate their positions can be expressed as follows:

$$P^i_{real} = [AP_{r1}, AP_{r2}, AP_{r3}, \ldots, AP_{rn}] \tag{2}$$

where AP_{rn} indicates a signal strength vector measured at the i position. With regard to each AP_{rn} of Eq. (2), the RSSI array is determined in the order of SSID set up automatically when the initial radio map is created with the RSSIs of each measured AP that matches each AP_n of Eq. (1). Here, RSSI that have not been measured are excluded from subsequent computations. All P^i on the radio map and P^i_{real} measured in real time are computed by Eq. (3).

$$Dist(i) = \sqrt{\sum_{j=1}^{n} (AP_j - AP_{rj})^2} \tag{3}$$

where AP_j denotes the RSSI of the identical SSID on the radio map, and AP_{rj} denotes that of the identical SSID measured in real time. The $Dist(i)$ value obtained from this computational step based on Euclidean distance has an eigenvalue for each position i. Because P^i_{real} is a value measured at the position of a mobile object, the AP number and signal intensity continue to change because they are measured in accordance with the state and location of the receiver. Because P_s has the most similar RSSI among the $Dist(i)$ values iteratively computed according to the number of i, i.e., the smallest $Dist(i)$, it can be obtained by Eq. (4).

$$P_s = arg\,min(Dist(i)) \tag{4}$$

where *arg min* denotes the minimum quantity. In other words, the minimum value i is sought from among all $Dist(i)$ values in this operation step. This i is set as the final location Ps of the mobile object.

Figure 1 shows the characteristic experiments of RSSI collection in indoor and outdoor environments of a building. Here, the X axis and Y axis refer to the measured average

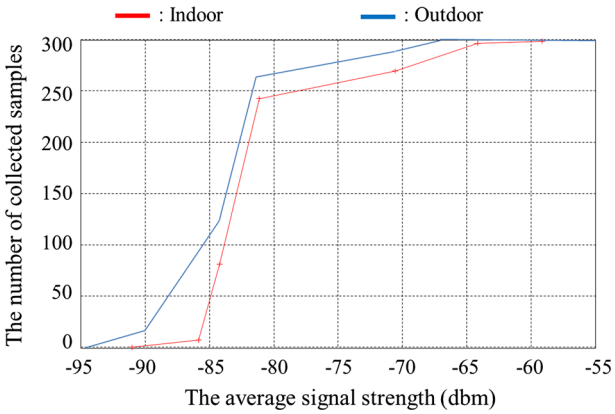

Fig. 1 The characteristic experiments of collected RSSI in indoor and outdoor environments of a building

signal strength and the number of measurement count, respectively. The multiple paths that cause propagation losses are practically inevitable in indoor environment due to four phenomena: diffraction, scattering, reflection and refraction. Here, we can see that the signal acquisition of indoor building is more difficult owing to obstacles than outdoors.

Figure 2 shows the characteristic experiments of Wi-Fi RSSI in the corridor of a ship and a building. Here, the *X* axis refers to the distance between Wi-Fi transmitter and receiver; the *Y* axis refers to the measured RSSI. Generally, a building and a ship consist of concrete and steel, respectively.

Therefore, we can see that wave reflection is largely generated in indoor environment of ship than building environment due to the size of indoor space and the steel structures. As a result, this problem in a ship is represented that the attenuation rate according to distance is weakly decreased compared with other environments. Because of these result, most of fingerprint depending on the attenuation of the signal is difficult to apply in the ship [16, 17]. Therefore, in order to apply positioning system to a ship, a modified fingerprint technique is required.

2.2 UWB-Based Positioning

Because UWB has a high-time resolution and high-speed data transmission given the broad UWB range between 3.5 and 10.6 GHz using *ns*-level impulse radio, UWB has broad application fields other than positioning, such as high-speed data transmission. UWB transmitter and receiver units deliver extremely accurate distance estimations with cm-level errors, even in multipath environments. UWB uses a peer-to-peer two-way time-of-flight (TW-TOF) ranging method between nodes, and thus has a smaller error range of measured values compared to other positioning-related communication methods. Figure 3 shows UWB-based TW-TOF range measurement applications.

The distance *R* between Anchor A and Anchor B is estimated as follows:

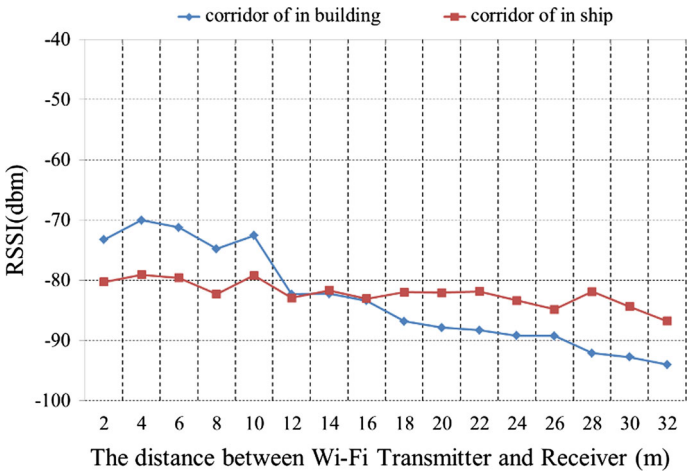

Fig. 2 The characteristic experiments of Wi-Fi RSSI in the corridor of a ship and a building

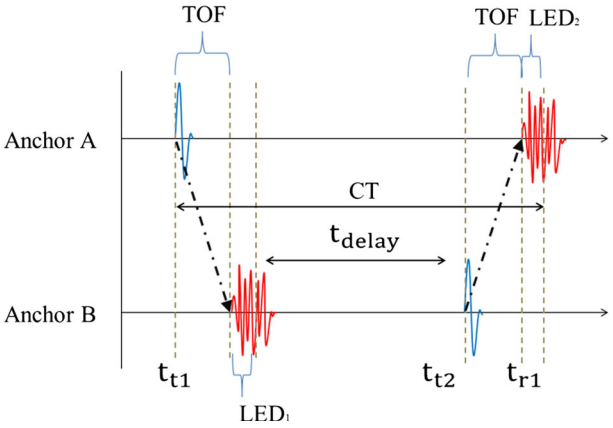

Fig. 3 UWB two-way TOF range measurement

$$R = TOF_{AB} \times C$$
$$TOF_{AB} = \frac{1}{2}(CT - T_{delay} - LED_1 - LED_2) \tag{5}$$

where TOF_{AB} is the average time measured by TOF between two nodes twice to enhance accuracy, CT is the total time required to complete the TOF_{AB} process between Anchor A and Anchor B, T_{delay} is the time delay depending on the anchor process speed, the leading edge detection (LED) represents the detection time of direct path required for the waveform analysis to differentiate a direct path from a multipath when signals are received over a direct path and multipath. Finally, the node-to-node distance R is obtained by multiplying the speed of light C to convert the measured time TOF_{AB} into distance [18, 19].

As shown in Fig. 4, the data of Wi-Fi and UWB received from APs is transmitted over a serial communication to MCU (microcontroller unit). Among many parameters included in the physical layer of UWB, the MCU is received only the necessary parameter values such as Node ID and distance through the serial communication which is a relatively simple

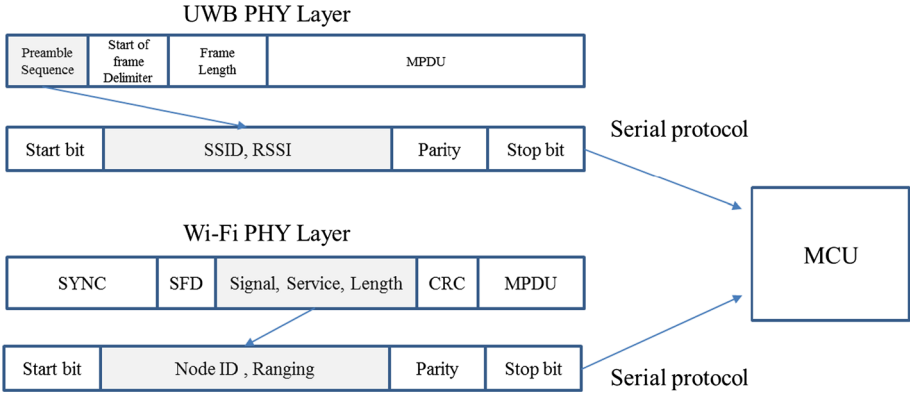

Fig. 4 Data transfer of received signals through serial protocol

method compared to other data transfer methods. Thus, the necessary parameter values are collected through each serial port.

Generally, UWB system, based on TOA techniques and frequency analysis plus owing to its high permeability, is robust against the NLOS environment with obstacles and offers higher accuracy. However, the price of this high performance positioning system is also high. Therefore, in terms of expected cost savings, it is difficult to cover all areas of ship using only UWB.

3 Proposed Method for Shipboard Precision Positioning and Automatic Updating

Here we demonstrate that the proposed system can reduce the number of UWB nodes and improve the network communication environment through combining UWB and the Wi-Fi network which is installed on a ship. Also, the proposed algorithm is implemented by considering of the signal variation and the spatial structure of ship, unlike most conventional methods which are focused on land environment. The positioning system proposed in this study uses a fingerprint-type Wi-Fi positioning and UWB system, and is thus divided into two phases: training phase and positioning phase.

Figure 5 shows the data flowchart of proposed positioning system. In the training phase to create the modified radio map based on UWB and Wi-Fi signals, all Wi-Fi signals installed in an experimental area of a ship are scanned through a designed smartphone App. In the scanning process, the APs of UWB are installed at the optimal location to enhance the positioning accuracy and then the weak RSSIs of Wi-Fi with insufficient reliability and irregular reception of signals are removed by adaptive thresholding step. After that, the modified radio map is created in MYSQL. In the positioning phase, the real positions of user are estimated by using modified radio map stored in MYSQL and these positions are measured by manufactured hardware that can be collected Wi-Fi and UWB signals. Also,

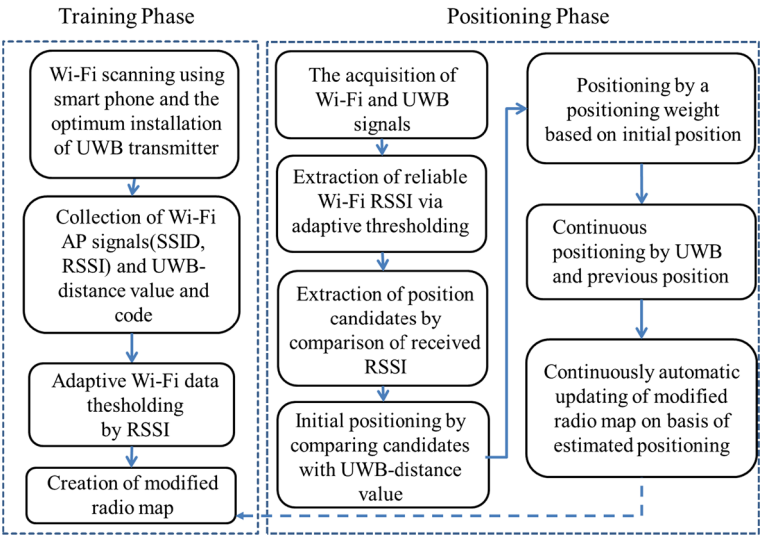

Fig. 5 Data flowchart for proposed system

the first position is estimated through Wi-Fi and UWB, and the other positions thereafter are estimated by using only UWB. The system architecture for implementing the proposed system is shown in Fig. 6a. First, we identify the Wi-Fi network in the experimental area in which location tracking is performed and constitute two-tiered hardware to create a modified radio map, as shown in Fig. 6b. Here, we used an android-based smartphone developed by HTC as the mobile node of a mobile object for RSSI measurement and used Time Domain's RCM410 for UWB distance estimation.

The RSSI measured with the smartphone is transmitted via Bluetooth, and the distance values estimated from UWB are transmitted to MCU (Atmega128) placed at the bottom of the hardware board via RS232 transmission. Each data-collection cycle is 0.5 s and the RSSI of Wi-Fi, which is collected each time the mobile node moves 1 m based on the value measured from UWB, is recognized as the RSSI of the estimated position and automatically inputted to the MYSQL of the server computer via Bluetooth. The radio map created in MYSQL is expressed as Eq. (6) by adding the distance and signal information of UWB to the AP signals collected by Eq. (1)

$$MOD\_P^i = \begin{bmatrix} AP_1, AP_2, AP_3, \ldots, AP_n, \\ UWB\,code,\ distance\,value \end{bmatrix} \tag{6}$$

In Eq. (6), because this *UWB code* is the unique number of each UWB fixed node for identifying the nodes, prior to Euclidean computation, a total amount of computation can be reduced by this code matching process which can extract only the same code value. Also, using this *distance value* measured between the fixed node and the mobile node, the positions of objects placed in sections difficult to distinguish can be identified and mobile objects can be tracked. And the modified radio map in the experimental area is a set which is created with the values MOD_P^i collected in accordance with each position i.

Conventional radio map stores not only the RSSIs of the measured AP signals, but also the quantified signal changes that may occur at the corresponding reference points, such as minimum and maximum values and standard deviations [20]. The RSSI stored in a created radio map is continuously updated by using related devices, such as GPS and geomagnetic sensors, in order to adjust the RSSI changing in accordance with the move or removal of

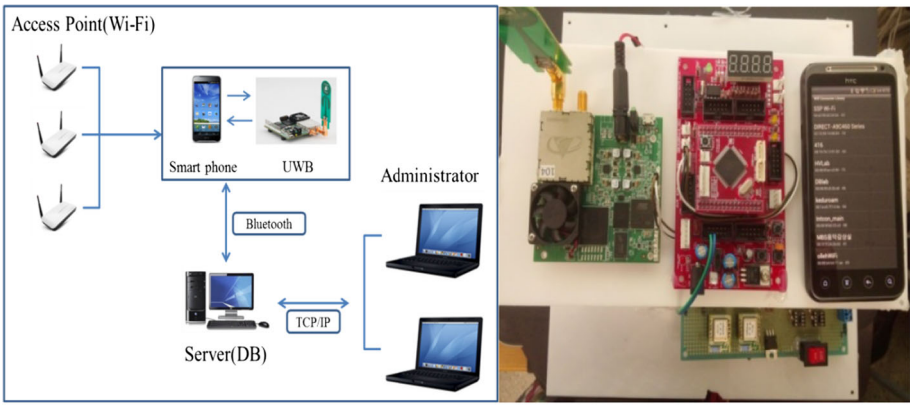

Fig. 6 **a** System architecture and **b** hardware for receiving Wi-Fi and UWB signals of the proposed algorithm

APs. These updating methods deteriorate accuracy over time because of the accumulated errors relative to the operation duration of sensors and the signal distortion-induced errors. In particular, because ships in an emergency situation require high-precision positioning for the safety of crew and passengers, these methods that incur accumulated errors are difficult to be applied on shipboards.

However, by using the proposed modified radio map, the estimation errors can be substantially reduced and the automatic updating and rapid implementation of radio map, which are difficult to be implemented by conventional methods [21], are possible. In the positioning phase, the final position of a mobile object is determined by comparing the measured signals with the modified radio map created in the training phase. First, the adaptive thresholding is performed to retain only reliable signal ranges from the Wi-Fi-based RSSIs measured at the position of the mobile object. The applied thresholding value is calculated with Eq. (7) established experimentally on the basis of the experimental results from a previous study [22].

$$\begin{aligned} P_r^i &= [AP_{r1}, AP_{r2}, AP_{r3}, 3, AP_{rn}] \\ AP_{rn} &= 0 \quad if \quad -100\,\text{dbm} > AP_{rn} > -80\,\text{dbm} \end{aligned} \tag{7}$$

where P_r^i is the RSSI measured with a smartphone, whereby the RSSI of AP_{rn} measured between -80 and -100 dbm is considered to be zero, and thus excluded from the subsequent Euclidean computation process. This adaptive thresholding process aims to reduce computational burden compared to conventional algorithms by performing comparative computation using only reliable signals that exhibit strong signal intensities and by removing all signals which are difficult to measure because of signals weakened by obstacles such as corridor, walls, and other structures, and to perform the seamless multi-object tracking. In particular, if fingerprint is implemented by using a smartphone, large signal fluctuations occur even at one position because of surrounding obstacles and low performance of Wi-Fi receivers, with weak RSSI ≤ -80 dbm which is hardly measurable. Therefore, in the case of a wide area to be measured with a large-size radio map, Euclidean computation is performed on the Wi-Fi-based RSSI trimmed by taking the adaptive thresholding in a specified area estimated by the UWB code. However, even if this Euclidean computation on a specified area is performed, the result can yield two or three candidate positions instead of tracking the final position of the mobile object, which can be tracked by approximating the real position and interpreting the state of signal reception. Figure 7a, b show the estimated positions without using UWB and Fig. 7c, d with using UWB in the corresponding position of Fig. 7a, b when measuring a total of 6 times in two positions of the experimental area, respectively. Here, the red circles indicate the measured position that is expected to be a mobile object and the number in circles represents the number measured at that position. In the Fig. 7a, even if three expected candidate positions are represented as one point measured four times at the correct position and two points measured one time at the incorrect position, we can easily predict the correct position via the frequency number of the measured position. But, in the Fig. 7b, it is difficult to predict the correct position because two measured points have the same frequency number. This reason comes from that even if the location is different in the ship environment which is largely generated wave reflection due to the steel structure and narrow aisle, a similar signal can be measured. However, as shown in Fig. 7c, d, the proposed method with using UWB can distinguish the correct position by using a distance value of the UWB.

Therefore, the final position can be determined by distance-dependent discrimination of candidate positions as shown in Eq. (8).

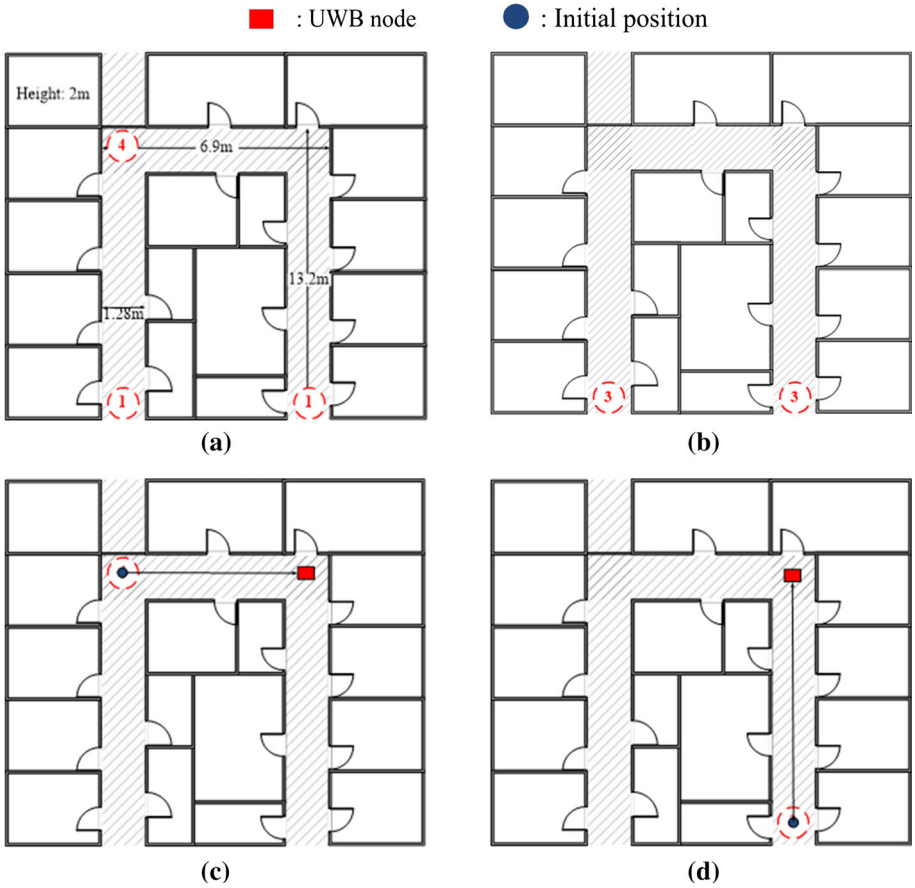

Fig. 7 Extraction of expected candidate positions without and with using UWB. **a** and **b** show the estimated positions without using UWB. **c** shows the extraction of expected positions with using UWB in cased of **(a)**. **d** shows the extraction of expected positions with using UWB in case of **(b)**

$$\begin{aligned} &if\ P_e = [P_{s1}, P_{s2}, \ldots, P_{sn}] \\ &P_s = \min(|P_{s1} - UWB\ distance\ value|, |P_{s2} - UWB\ distance\ value|, \ldots \\ &\quad |P_{sn} - UWB\ distance\ value|), \end{aligned} \tag{8}$$

where P_e is the set of estimated position values and P_s is the initial position value determined by the modified radio map.

Once the position of the mobile object is determined by the initially estimated position, the position can be continuously estimated by using the distance value of the UWB and a positioning weight without any use of modified radio map. Here, the final position value (P) can be expressed as Eq. (9)

$$\begin{aligned} &P = \alpha P'_s + (1-\alpha)P_m \\ &\quad if\ P_m - n < P'_s < P_m + n \end{aligned} \tag{9}$$

where α represents the positioning weight, P'_s is the latest estimated position value, P_m is the present estimated position value, n is a fixed value set up in order to prevent erratic

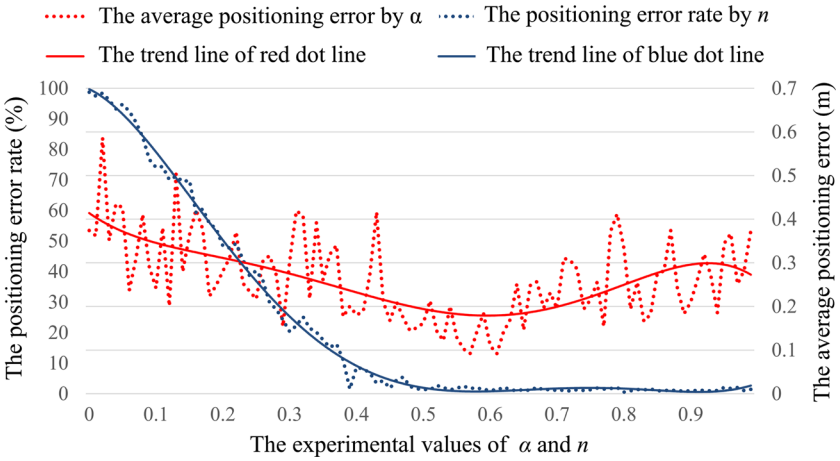

Fig. 8 The positioning effects on α and n values

localization between the direct path and multipath from among the positions yielded by P'_s. Figure 8 represents the positioning effects on n and α values to select their optimized values for more precise estimation. Here, the greater the value of n, the range of allowable error is also wider. So n and α are adapted as 0.5 m and 0.6 according to the trend line, respectively. If the previous position P'_s does not satisfy Eq. (9), the estimated position is considered wrong and positioning is repeated using Eq. (8). Also, at the final position value, if the Wi-Fi-based RSSI, which is included in the modified radio map, is different or doesn't exist, the measured RSSI is automatically and continuously updated to that of the modified radio map to adapt to rapid changes of AP position moves or indoor environments such as opening and closing doors in a ship.

4 Experimental Results

Experiments were carried out in order to verify the performance of the proposed algorithm in the Hanbada, the training ship of the Korea Maritime and Ocean University. We selected the experimental area with ship corridor(height 2 m, width 1.8 m) in which a lot of wave scattering and distortion can be occurred because of narrow area and several cabins, as shown in Fig. 9. Here, the WLAN reference points along the corridor section are indicated with black points. The experiments were started with the creation of a radio map, and each position was determined and measured under the condition of unknown WLAN installation position. All watertight or standard doors in the ship are made of steel so that wireless radio waves are interfered and the experiment of preliminary radio wave confirmed that WLAN and UWB signals are not received in these obstacles.

Accordingly, UWB was installed in an optimal point of an NLOS environment with a transmission distance of approximately 20 m based on a nine-channel model that is, in turn, based on the IEEE802.15.4a module [23, 24]. Each fixed UWB node was given a unique code that allowed for position identification so that an approximate estimation of the transmission area could be performed easily using the received UWB signals. The nodes were attached to the 2-m-high ceiling of the ship in order to minimize signal attenuation induced by a mobile object.

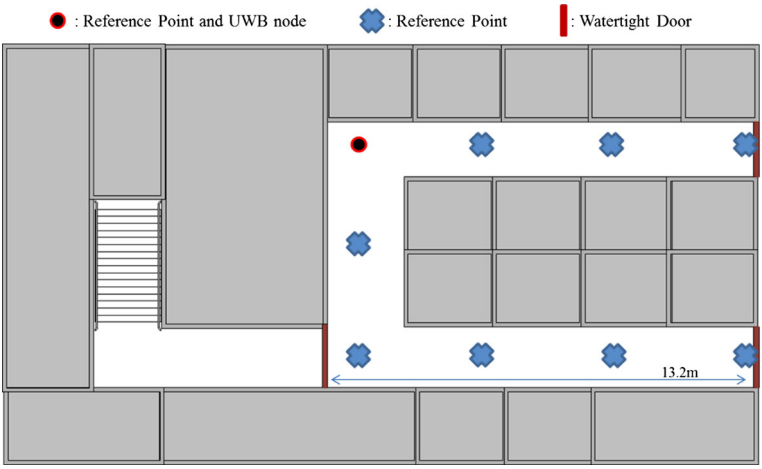

Fig. 9 The arrangement of reference points and UWB node in the experimental area

Also, all relevant factors, including the presence or absence of a watertight door and the UWB transmission distance, were integrally considered into the design of the node arrays; thus allowing signal reception in all open and closed spaces. For Wi-Fi RSSI reception, reference points were set up at 3-m intervals under the condition of unknown AP positions in the surrounding areas to be measured. Previous studies using TOF-based techniques estimated positions based on trilateration or bilateration that are required three or two fixed nodes, respectively. However, the proposed positioning method can be performed using only one fixed node considering the peculiarity of the ship's narrow corridor area. In the experimental process, the reference points from which Wi-Fi RSSI were collected were divided into 11 points, and the modified radio map is configured to automatically collect the Wi-Fi RSSI and the UWB code and distance values of UWB measured by 3 m interval. Also, considering energy consumption with other two methods (trilateration, bilateration), the power consumption of proposed method is saved 62 % compared to the trilateration method, 43 % compared to the bilateration method. Here, the average power consumption of Wi-Fi and UWB used in the experiment are 120 mW and 4.2 W, respectively. Table 1 shows the comparison of computational complexity. K is the amount of the Euclidean distance computation and T is the number of measurements according to operation time. Assuming that the same radio map is used, the computational complexity rapidly increases in fingerprint according to T while that rapidly decreases in the proposed algorithm after the initial K computation is performed. Therefore, the longer the operation time, the proposed algorithm can further reduce computational complexity than fingerprint and trilateration.

Table 1 The comparison of computational complexity

Measurement method	Computational complexity
Fingerprint	K*T
Trilateration	4T
Proposed algorithm	K + T

Table 2 The comparison of inertial sensor and UWB

Positioning error	Smartphone inertial sensor (m)	UWB (m)
Average	5	0.1
Maximum–minimum error range	10–3	0.3–0.01

Table 2 indicates the results of the comparison of the positioning errors between the radio map production methods using an inertial sensor [11] and UWB in the proposed system. In the method that uses an inertial sensor, a radio map was updated on the basis of incorrect positions because of the accumulated errors that occurred in proportion to the increasing distance, because this method relies on values measured by the sensor moving from position to position [25, 26]. However, in terms of the initial positioning accuracy, although the method using the inertial sensor is more accurate compared with the proposed algorithm, it should set the initial starting position manually and then the cumulative errors occur rapidly due to the intense magnetic energy in steel structure while any of them does not occur in the proposed algorithm over time. Consequently, even if the initial radio map consists of correct position data, the accuracy is reduced by RSSI changes caused by Wi-Fi position changes or interior structural changes. This can be remedied by adjusting the modified radio map on the basis of the accurate data yielded by UWB-based measurement, so that a new RSSI survey is not required.

Figure 10 shows the positioning accuracy rates obtained by varying adaptive thresholding values. The *X* axis refers to the configured point at 3-m intervals for signal acquisition; the *Y* axis refers to the accuracy of positioning. Among the RSSI measured in the range between −50 and −100 dbm, the values collected at −80 to −100 dbm have signals that are too weak to be influential in positioning. The adaptive thresholding of the signals between −70 and −80 dbm greatly influenced positioning. Therefore, it is verified that reducing fingerprint computational burden using only the RSSI between −80 and −50 dbm does not significantly influence the results and the maintenance of the accuracy. Table 3 outlines the experimental results by comparing the results yielded by trilateration, bilateration, and the proposed method. The mean positioning error of proposed method increased by approximately 0.06 m compared to the trilateration method; still, accuracy improves considerably compared to conventional methods. In addition, the proposed

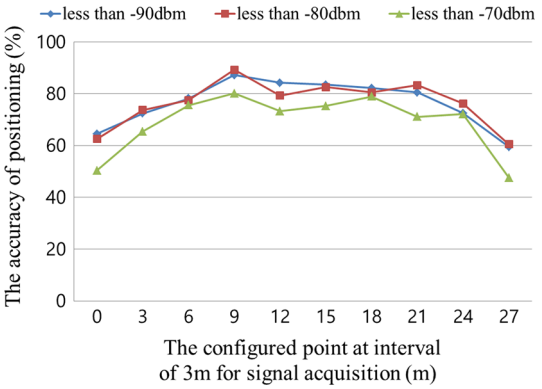

Fig. 10 The positioning accuracy according to the adaptive thresholding of RSSI

Table 3 Comparison of shipboard positioning errors by the number of fixed nodes

Method (the number of fixed node)	Trilateration (3) (m)	Bilateration (2) (m)	Proposed method (1) (m)
Mean positioning error	0.059	0.064	0.120

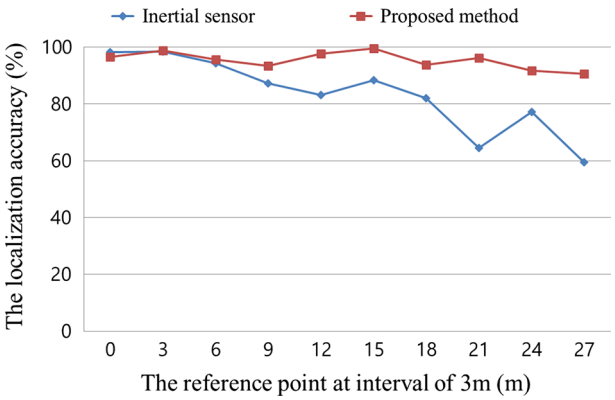

Fig. 11 Accuracy of measured localization according to reference point in a ship

method used only one node in terms of expected cost savings for UWB node within the same experimental area. Generally, because UWB and Wi-Fi are capable of receiving to five times per second, the accuracy of the data reception is reduced about 37.18 % owing to the multipath and errors. Therefore, the proposed algorithm is limited to 2 reception count per second for stable data reception. As a result, it occurs an average delay time of 0.27 s than when receiving at the maximum speed. In addition, even if, when the proposed device is initially operated, the delay time to access the modified radio map of 0.34 s occurs approximately compared with trilateration and bilateration, no longer exists except the initial operation. Figure 11 shows graphs that compare the experiment with an inertial sensor and that which applies the proposed method. This experiment was conducted to determine positioning accuracy, at each reference point(X), of the values(Y) obtained from ten different positions within the same experimental area. The values acquired by the inertial sensor show high accuracy rate during the initial stages; however, as the number of experiments is increased, position accuracy is decreased because of accumulated errors. The experiment results with UWB show errors that caused by using only one node, but the exact position could be constantly measured without the occurrence of cumulative errors. As a result, the proposed algorithm shows and average accuracy of 95.39 % while the inertial sensor shows an average accuracy of 83.52 %.

5 Conclusions

This paper presents a high-precision positioning and updating system using the Wi-Fi network available on shipboards and UWBs. The proposed method for shipboard high-precision positioning and updating accomplished several improvements compared with conventional methods. The proposed algorithm fused UWB and Wi-Fi can be compensated

using UWB in the ship area which is difficult to estimate the positioning by the existing fingerprint method. Not only does the proposed method show the positioning performance similar to trilateration and bilateration based on UWB, but it reduces the computational complexity due to removing the Euclidean distance process of fingerprint except only initial positioning. The validity of the proposed method was established by experiments performed in a ship where signals are easily distorted because of scattering and reflection of radio waves. A special merit of the proposed method is the simplification of selective radio map creation and rapid computation through the adaptive thresholding process. Even considering the error caused by reducing the number of node that requires high cost, the proposed method is a considerably improved performance compared to conventional Wi-Fi-based methods (error range: 2–3 m) and the modified radio map updating accuracy was also improved by 11.87 %. Also, Furthermore, the updating-related accuracy problem of conventional methods was resolved by automatic updating based on accurate positions that immediately reflect the changes of RSSIs acquired from AP without the need for manual corrections of the radio map once the initial radio map is established.

Acknowledgments This research was supported by Basic Science Research Program through the National Research Foundation of Korea (NRF) funded by the Ministry of Education (No. 2014R1A1A4A01008081).

References

1. Swangmuang, N., & Krishnamurthy, P. (2008). Location fingerprint analyses toward efficient indoor positioning. In *Sixth annual IEEE international conference on pervasive computing and communications*, pp. 101–109.
2. So, J. M., Lee, J. Y., Yoon, C. H., & Park, H. J. (2013). An improved location estimation method for Wi-Fi fingerprint-based indoor localization. *International Journal of Software Engineering and Its Applications, 7*(3), 77–86.
3. Arai, K., & Tolle, H. (2013). Color radiomap interpolation for efficient fingerprint WiFi-based indoor location estimation. *International Journal of Advanced Research in Artificial Intelligence, 2*(3), 10–15.
4. Fallah, N., Apostolopoulos, I., Bekris, K., & Folmer, E. (2013). Indoor human navigation systems: A survey. *Interacting with Computers, 25*(1), 21–33.
5. Zhou, Y., Jin, L., Jin, C., & Zhou, A. (2013). FIMO: A novel WiFi localization method. In *Asia-Pacific web conference* (pp. 437–448). Berlin: Springer.
6. Li, Y., & Liu, X. (2014). An indoor three-dimensional positioning algorithm based on difference received signal strength in WiFi. In *Computer engineering and networking: Proceedings of the 2013 international conference on computer engineering and network* (pp. 115–124). Springer Science & Business Media.
7. Chen, L., Li, B., Zhao, K., Rizos, C., & Zheng, Z. (2013). An improved algorithm to generate a Wi-Fi fingerprint database for indoor positioning. *Sensors, 13*(8), 11085–11096.
8. Kim, Y. G., Chon, Y. H., & Cha, H. G. (2012). Smartphone-based collaborative and autonomous radio fingerprinting. *IEEE Transactions on Systems, Man, and Cybernetics Part C: Applications and Reviews, 42*(1), 112–122.
9. Dil, B. J., & Havinga, P. J. M. (2010). RSS-based localization with different antenna orientations. In *Australasian telecommunication networks and applications conference*, pp. 13–18.
10. Fan, R., Tian, Z., Linfu, D., Li, J. Y., & Wan, Q. (2010). Indoor localization error measurements with multiple channels. In *2010 second international conference on networks security, wireless communications and trusted computing*, Vol. 2, pp. 176–179.
11. Manodham, T., Loyola, L., & Miki, T. (2008). A novel wireless positioning system for seamless internet connectivity based on the WLAN infrastructure. *Journal of Wireless Personal Communication, 44*(3), 295–309.
12. Qiu, J., Wang, X., & Dai, G. (2014). Improving the indoor localization accuracy for CPS by reorganizing the fingerprint signatures. *International Journal of Distributed Sensor Networks, 415710*, 2014.
13. Liu, H., Wang, Y., Chen, Y., Yang, J., Sidhom, S., & Ye, F. (2014). Accurate WiFi based localization for smartphones using peer assistance. *IEEE Transactions on Mobile Computing, 13*(10), 2199–2214.

14. Muller, P., Wymeersch, H., & Piche, R. (2014). UWB positioning with generalized Gaussian mixture filters. *IEEE Transactions on Mobile Computing, 13*(10), 2406–2414.
15. Saeed, A., Kosba, A. E., & Youssef, M. (2014). Ichnaea: A low-overhead robust WLAN device-free passive localization system. *IEEE Journal of Selected Topics in Signal Processing, 8*(1), 5–15.
16. Sarkar, A., Majumdar, S., & Bhattacharya, P. P. (2013). Path loss estimation for a wireless sensor network for application in ship. *International Journal of Computer Science and Mobile Computing, 2*(6), 87–96.
17. Pena, D., Feick, R., Hristov, H. D., & Grote, W. (2003). Measurement and modeling of propagation losses in brick and concrete walls for the 900-MHz band. *IEEE Transactions on Antennas and Propagation, 51*(1), 31–39.
18. Dewberry, B., & Beeler, W. (2012). Increased ranging capacity using ultrawideband direct-path pulse signal strength with dynamic recalibration. In *Proceedings of the 2012 IEEE/ION position, location and navigation symposium*.
19. Johnson, J., & Dewberry, B. (2011). Ultra-wideband aiding of GPS for quick deployment of anchors in a GPS-denied ad-hoc sensor tracking and communication system. In *Proceedings of ION GNSS*.
20. Lim, J. S., Jang, W. H., Yoon, G. W., & Han, D. S. (2013). Radio map update automation for WiFi positioning systems. *IEEE Communications Letters, 17*(4), 693–696.
21. Kim, J. Y., Ji, M. I., Cho, Y. S., Lee, Y. K., & Park, S. J. (2013). Fingerprint DB generating system exploiting PDR based dynamic collection for indoor localization of smart-phone users. In *IEEE 2013 13th international conference on control, automation and systems (ICCAS)*, pp. 715–718.
22. Youssef, M., Agrawala, A., & Shankar, A. U. (2003). WLAN location determination via clustering and probability distributions. In *Proceedings of the first IEEE international conference on pervasive computing and communications*, pp. 143–150.
23. Molisch, A. F., Balakrishnan, K., Chong, C. C., Emami, S., Fort, A., Karedal, J., et al. (2004). *IEEE 802.15. 4a channel model-final report*. IEEE.
24. Park, J. G., Charrow, B., Curtis, D., Battat, J., Minkov, E., Hicks, J., et al. (2010). Growing an organic indoor location system. In *Proceedings of the 8th international conference on mobile systems, applications, and service*, pp. 271–284.
25. Gallagher, T., Li, B., Dempster, A. G., & Rizos, C. (2010). Database updating through user feedback in fingerprinting-based Wi-Fi location systems. In *Ubiquitous positioning indoor navigation and location based service*, pp. 1–8.
26. Hossain, A. M., Van, H. N., & Soh, W.-S. (2010). Utilization of user feedback in indoor positioning system. *Pervasive and Mobile Computing, 6*(4), 467–481.

Ju-Hyeon Seong He received his B.S. and M.S. degrees in electrical and electronics engineering from Korea Maritime and Ocean University, South Korea, in 2012 and 2014, respectively. He is currently pursuing the Ph.D. degree in electronics engineering at Korea Maritime and Ocean University. His research interests include positioning system, sense network and embedded signal processing.

Eun-Chang Choi He received his B.S., M.S., and Ph.D. degrees in electronic engineering from Kyungpook National University, South Korea, in 1990, 1992, and 2006, respectively. Since 1993, he has been with Electronics Telecommunications Research Institute, where he is currently a director in the Section of Medical IT Convergence Research. His research interests include WPAN, IoT, and Medical Robotics.

Jang-Se Lee He received the B.S., M.S., and Ph.D. degrees in Computer Engineering from Korea Aerospace University in 1997, 1999, and 2003 respectively. During Jan. 2013–Jan. 2014, He stayed in Duke High Availability Assurance Lab (DHAAL), Duke University as a visiting scholar. He is currently an associate professor (from 2004) in the division of Information Technology, Korea Maritime and Ocean University. His research interest includes modeling and simulation, intelligent systems, security for systems and networks, system survivability, and E-navigation.

Dong-Hoan Seo He received his B.S., M.S., and Ph.D. degrees in electronic engineering from Kyungpook National University, South Korea, in 1996, 1999, and 2003, respectively. Since 2004, he has been with Korea Maritime and Ocean University, where he is currently a professor in the Division of Electronics and Electrical Information Engineering. His research interests include sense network, signal processing, and computer vision.